Optimised GTO-GEO Transfer Using Low-Thrust Propulsion

By Marilena DI CARLO,[1)] Massimiliano VASILE,[1)] and Stephen KEMBLE[2)]

[1)]*Department of Mechanical and Aerospace Engineering, University of Strathclyde, Glasgow, United Kingdom*

[2)]*Airbus Defence and Space, Stevenage, United Kingdom*

(Received April 17th, 2017)

This paper proposes a global optimisation of the low-thrust transfers from GTO to GEO incorporating different types of perturbation. The trajectory transcription method makes use of an analytical solution of the perturbed Keplerian motion together with a simple direct collocation of the thrust arcs. The paper will show that low-thrust GTO to GEO transfers exhibit a number of local minima with a small but not negligible difference. The paper presents different strategies to explore the set of local minima and shows a number of locally optimal solutions.

Key Words: GTO-GEO transfer, electric propulsion, trajectory optimisation

1. Introduction

In this work an optimal electric propulsion transfer from Geostationary Transfer Orbit (GTO) to Geostationary Equatorial Orbit (GEO) is studied. Electric propulsion has been used since mid-1997 for the station keeping of Geostationary satellites.[8)] More recently, in March 2015, two Boeing all-electric satellites performed for the first time an electric-propelled orbit raising to the Geostationary Equatorial Orbit*. Low-thrust trajectories are indeed an efficient alternative to chemically propelled ones, since they have the potential to provide increased mass delivered to destination and smaller launch vehicles.[15)]

Several works in the literature have studied methods to optimise the transfer of spacecraft from GTO to GEO. Kluever[6)] uses a direct optimisation method to solve the GTO-GEO transfer. The weights to three optimal feedback control laws (for the variation of semimajor axis, eccentricity and inclination) are obtained as solution of a non-linear programming problem (NLP) in which the objective is the minimisation of the time of flight. The trajectory is propagated using orbital averaging and including perturbations from Earth shadows, oblateness and solar cell degradation. The same author also studied the GTO-GEO transfer with variable specific impulse.[7)] In this case the costates time histories are parametrised by linear interpolation and the design variables of the NLP are the nodal values of the costates. The objective is the minimisation of the fuel mass and a local optimisation method is used to solve the problem. Graham studied a direct method transcribed using GPOPS-II and solved using IPOPT, with analytical first and second derivatives computed by means of the software ADiGator.[5)] These methods, and the methods traditionally used to optimise low-thrust trajectories, are local methods. As such, they are able to find *a* solution, not *the best* solution.[2,13)] Moreover, the NLP methods require an initial guess that is not only hard to find but that also generally causes the optimiser to converge to an optimal trajectory close to the initial guess (that is rarely close to the global optimum).[2)] To overcome the limitation of local optimisation methods, effective global optimisation techniques are required. Global optimisation of low-thrust trajectory in the literature mainly focuses on the optimisation of interplanetary transfers.[2,9,16)]

In this work a global optimisation technique is applied to the GTO-GEO low-thrust transfer. The objective is the minimisation of the fuel consumption for the GTO-GEO transfer in a given time of flight. During the transfer the thrust is applied on two or four thrust arcs, two of which are centred at the perigee and apogee of the transfer orbits. The control parameters are the length of the thrust arcs and the elevation angle of the low-thrust vector. A population-based stochastic global optimisation algorithm, Multi-Population Adaptive Inflationary Differential Evolution Algorithm (MP-AIDEA),[3)] is used to globally explore the search space, and no user-defined initial guess is required to start the optimisation process. The model used for the motion of the spacecraft is an analytical propagator,[17)] which speeds up the optimisation process with respect to the use of a numerical one. The analytical propagator is based on non-singular equinoctial elements and includes low-thrust acceleration and perturbations due to Earth's zonal harmonics J_2, J_3, J_4, J_5, atmospheric drag and third body gravitational perturbation from the Sun. Preliminary results show that many local minima exist for the solution of the minimum fuel low-thrust GTO-GEO problem. The paper starts with the description of the problem and of MP-AIDEA in Section **2.**. The optimal transfer is studied with no perturbations in Section **3.** and with the perturbations due to Earth's oblateness, drag and Sun gravitational attraction in Section **4.**. Section **5.** concludes the paper.

2. The GTO-GEO global optimisation problem

This paper is concerned with the global optimisation of transfers from GTO to GEO with initial and final orbital parameters defined in Table 1. In Table 1, a, e, i, Ω, ω are the semimajor axis, eccentricity, inclination, right ascension of the ascending node and argument of the perigee. The nominal time of

Table 1. GTO and GEO orbital elements.

	a [km]	e	i [deg]	Ω [deg]	ω [deg]
GTO	24505	0.725	7	0	0
GEO	42165	0	0	-	-

* http://boeing.mediaroom.com/2015-09-10-Boeing-World-s-First-All-Electric-Propulsion-Satellite-Begins-Operations

flight for the transfer is $ToF = 225$ days. The spacecraft has initial mass $m_0 = 2000$ kg and engine characterised by thrust $T = 0.5$ N and specific impulse $I_{sp} = 2000$ s. The thrust vector is defined by its magnitude ϵ and by its azimuth and elevation angles, α and β, in a radial-circumferential-normal reference frame (RCN):

$$a_R = \varepsilon \cos\beta \sin\alpha,\ a_C = \varepsilon \cos\beta \cos\alpha,\ a_N = \varepsilon \sin\beta \quad (1)$$

Initially the thrust is applied along two arcs per orbital revolution, at the perigee and apogee of each orbit.[17] In the absence of perturbations and for the initial orbital elements given in Table 1, arcs centered at perigee and apogee represents ideal positions along the orbit to change semimajor axis, eccentricity and inclination. Considering the Gauss' equations expressing the time variation of semimajor axis and eccentricity due to perturbations,[1] it is possible to define the point of the orbit providing the maximum rate of change of a and e by computing:

$$\frac{\partial}{\partial\theta}\frac{da}{dt} = 0,\ \frac{\partial}{\partial\theta}\frac{de}{dt} = 0, \quad (2)$$

where θ is the true anomaly. The previous equations give $\theta_a = 0$ for the maximum rate of change of the semimajor axis and $\theta_e = \pi$ for the maximum rate of change of the eccentricity, showing indeed that thrusting arcs centered at perigee and apogee provide the maximum instantaneous variation of semimajor axis and eccentricity. Following a similar analysis, the point of the orbit providing the maximum rate of change of i is at true anomaly θ_i given by:[10]

$$\sin(\theta_i + \omega) = -e \sin\omega \quad (3)$$

Fig. 1 shows θ_i as a function of ω ranging from 0 to 2π. Due to the arcsin term in Eq.(3), the optimal position to change i is at θ_i and $\theta_i + \pi$. Fig. 1 shows that when $\omega = 0$ and no perturbations

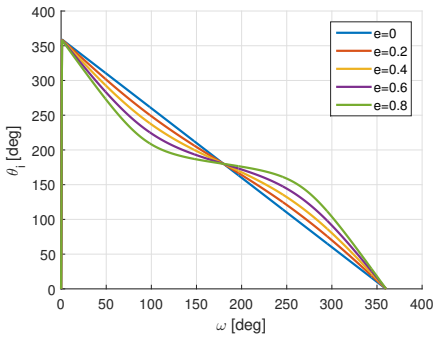

Fig. 1. θ_i providing the maximum rate of change of i as a function of ω and for different values of e.

causes ω to change, the perigee and apogee centered thrust arcs are ideal positions to change the inclination. However when ω changes or its initial value is not 0 or π, the positions along the orbit providing the maximum instantaneous rate of change of inclination are no more at perigee and apogee. For example, by considering the Gauss' equation for the inclination, in the limit case in which $\omega = 90$ deg and $\omega = 270$ deg, thrust applied at $\theta = 0$ and $\theta = 180$ deg results in zero variation of the inclination. In these cases two additional thrust arcs are added, for each revolution. This will be explained in Section **4.**. For the case without perturbation and with initial orbital elements defined in Table 1, two thrust arcs are considered. The length of the perigee arc is defined by the angle ΔL_p and the length of the apogee arc is ΔL_a. The parameters defining the problem are ΔL_p and ΔL_a and the elevation angle at perigee and apogee, β_p and β_a. The azimuth angle on the two thrust arcs is not optimised as it follows one of the following four strategies: (1) Tangential thrust on both perigee and apogee thrust arc; (2) Tangential thrust at perigee, $\alpha = 0$ at apogee;[8] (3) $\alpha = 0$ at perigee, tangential thrust at apogee; (4) $\alpha = 0$ on both perigee and apogee thrust arc.[8] The control parameters are discretised during the transfer by considering four nodes to model the variation of ΔL_p, ΔL_a, β_p and β_a from $t = 0$ to $t = ToF$. A linear interpolation is then used to define the value of the control parameters at any time during the transfer. The vector of parameters to optimise is defined, therefore, by 16 variables:

$$\begin{aligned}\mathbf{x} = [&\Delta L_{p1}\ \Delta L_{p2}\ \Delta L_{p3}\ \Delta L_{p4}\ \Delta L_{a1}\ \Delta L_{a2}\ \Delta L_{a3}\ \Delta L_{a4}\\ &\beta_{p1}\ \beta_{p2}\ \beta_{p3}\ \beta_{p4}\ \beta_{a1}\ \beta_{a2}\ \beta_{a3}\ \beta_{a4}]^T\end{aligned} \quad (4)$$

$\Delta L_{pi}, \Delta L_{ai}, \beta_{pi}, \beta_{ai}$ represents the value of the control parameters at node i. The state of the spacecraft is propagated using an averaged analytic propagator based on a first-order expansion of the perturbed equations of motion.[17] The propagation is realised using non-singular equinoctial elements. The optimisation problem consists in the minimisation of the ΔV required to realise to the transfer while constraining the final orbital elements at the end of the transfer to coincide with those of the GEO. The nonlinear constrained optimisation problem can be formulated as:

$$\begin{aligned}&\text{min. } f(\mathbf{x}) = \Delta V\\ &\text{s.t. } g_j(\mathbf{x}) \le 0 \quad j = 1,\dots,m\\ &\quad h_k(\mathbf{x}) = 0 \quad k = 1,\dots,l\\ &\quad x_i^L \le x_i \le x_i^U \ i = 1,\dots,n\end{aligned} \quad (5)$$

The equality constraints $\mathbf{h}(\mathbf{x})$ are:

$$\begin{aligned}h_1(\mathbf{x}) &= a(ToF)[1 - e(ToF)] - a_{GEO}\\ h_2(\mathbf{x}) &= a(ToF)[1 + e(ToF)] - a_{GEO}\\ h_3(\mathbf{x}) &= 10\left[\sqrt{Q_1(ToF)^2 + Q_2(ToF)^2} - \tan\left(\frac{i_{GEO}}{2}\right)\right]\end{aligned} \quad (6)$$

where $a(ToF)$, $e(ToF)$ are the semimajor axis and eccentricity at the end of the transfer and $Q_1(ToF)$ and $Q_2(ToF)$ are the third and fourth equinocital elements at the end of the transfer. a_{GEO} and i_{GEO} are the semimajor axis and inclination of the target GEO (Table 1). The constraint on the final inclination is multiplied by 10 in order to match more precisely the final inclination of the GEO. The disequality constraints $\mathbf{g}(\mathbf{x})$ are:

$$\begin{aligned}g_1(\mathbf{x}) &= R_\oplus - \min[a(t)(1 - e(t))]\\ g_2(\mathbf{x}) &= \max\left(\|\Delta L_p(t)\| + \|\Delta L_a(t)\|\right) - 2\pi\end{aligned} \quad (7)$$

They impose that the minimum perigee radius during the transfer is higher than the Earth's radius, $R_\oplus$, and that the maximum sum of perigee and apogee thrust arc length is lower than 2π. The lower and upper boundaries vectors are:

$$\begin{aligned}&x_i^L = -2\pi,\ x_i^U = 2\pi,\ \ i = 1,\dots,8\\ &x_i^L = -\pi/2,\ x_i^U = \pi/2,\ i = 9,\dots,16\end{aligned} \quad (8)$$

The stochastic global optimisation algorithm used in this study, MP-AIDEA, is not formulated to explicitly manage constraints. The constrained problem presented in Eq. (5) is therefore transformed into an unconstrained problem, applying a penalty method. The fitness function is expressed as a combination of the objective function and penalty constraints:

$$f'(\mathbf{x}) = f(\mathbf{x}) + w_1 \left[(\mathbf{g}(\mathbf{x}) > 0) \cdot |\mathbf{g}(\mathbf{x})|\right]^2 + w_2 |\mathbf{h}(\mathbf{x})|^2 \quad (9)$$

where w_1 and w_2 are appropriate weight coefficients. MP-AIDEA is a population-based evolutionary algorithm for solving single-objective global optimisation problems over continuous spaces. It combines adaptive Differential Evolution (DE),[11] with the restarting procedure of Monotonic Basin Hopping (MBH).[14] MP-AIDEA is able to automatically adapt the parameters of the DE and MBH during the optimisation. At the end of the DE a local search is run from the best individual of each population, and **the local search algorithm solves the problem defined in Eq. 5.** Using the restarting mechanism of MBH in combination with the DE, the populations are able to move, in a funnel structure, from one local minima to another, until the global minimum of the problem is located. MP-AIDEA implements also an approach to avoid multiple detection of the same local minima, by restarting the population in the entire work space when it falls within the basin of attraction of an already detected minimum. MP-AIDEA collects in an archive the local minima found during the exploration. It gives therefore the possibility to evaluate different possible solution to the GTO-GEO transfer problem, each one corresponding to a different local minimum.

3. GTO-GEO transfer without perturbations

In this section the optimisation of the GTO-GEO transfer, without perturbations, is presented. At first, local solutions to the problem are found using different initial guesses, based on a pre-defined structure for the initial guess vector $\mathbf{x}_0$.[17] The NLP problem presented in Eq. (5) is solved using MATLAB *fmincon-sqp*. MP-AIDEA is then used to globally explore the whole search space, using the fitness function defined in Eq. (9). For the local optimisation method, the vector of initial guess is:

$$\mathbf{x}_0 = [\Delta L_{p1,0}\ \Delta L_{p2,0}\ \Delta L_{p3,0}\ \Delta L_{p4,0}\ \Delta L_{a1,0}\ \Delta L_{a2,0}\ \Delta L_{a3,0}\ \Delta L_{a4,0}\ \beta_{p1,0}\ \beta_{p2,0}\ \beta_{p3,0}\ \beta_{p4,0}\ \beta_{a1,0}\ \beta_{a2,0}\ \beta_{a3,0}\ \beta_{a4,0}]^T \quad (10)$$

The initial guess is constructed using values of ΔL_{ai} linearly spaced from 0 to $\Delta L_{a4,0}$:

$$\Delta L_{ai,0} = \frac{\Delta L_{a4,0}}{3}(i-1), \quad i = 1, \ldots, 4 \quad (11)$$

The initial guess of the length of the perigee thrust arcs corresponding to the first three nodes is:

$$\Delta L_{p1,0} = \Delta L_{p2,0} = \Delta L_{p3,0} = 0 \quad (12)$$

while $\Delta L_{p4,0} \neq 0$. The initial guess for the elevation angles is:

$$\beta_{pi,0} = \beta_{ai,0} = 0, \quad i = 1, \ldots, 4 \quad (13)$$

Using Eq. (11), (12) and (13), the vector of initial guess $\mathbf{x}_0$ of Eq. (14) can be defined using only two parameters, $\Delta L_{p4,0}$ and $\Delta L_{a4,0}$:

$$\mathbf{x}_0 = [0\,0\,0\,-\Delta L_{p4,0}\,0\,\frac{\Delta L_{a4,0}}{3}\,\frac{2\Delta L_{a4,0}}{3}\,\Delta L_{a4,0}\,0\,0\,0\,0\,0\,0\,0\,0]^T \quad (14)$$

$\Delta L_i < 0$ correspond to thrust applied in the negative circumferential direction. Different values of $|\Delta L_{p4,0}|$ and $|\Delta L_{a4,0}|$ have been considered, in the range $[0, 180]$ deg, at interval of 10 degrees, resulting in a total of 100 local optimisation problems for the 4 thrusting strategies defined in Section **2.**. The results are shown in Fig. 2 to Fig. 5. Empty spaces in the plot represent conditions where the problem did not converge to a feasible solution using that initial guess. Results show that in all the

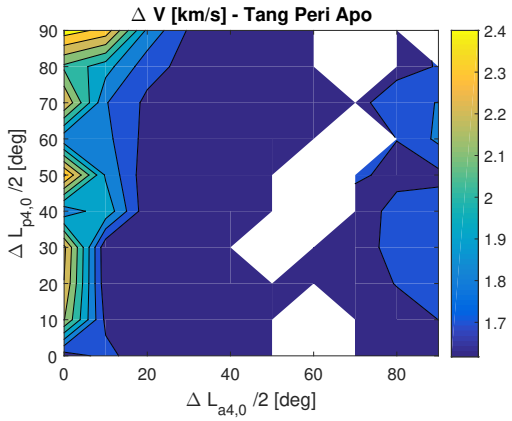

Fig. 2. ΔV for different initial guesses of $\Delta L_{a4,0}$ and $\Delta L_{p4,0}$, Strategy 1.

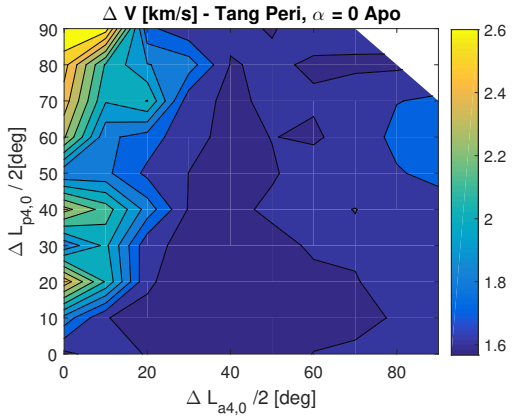

Fig. 3. ΔV for different initial guesses of $\Delta L_{a4,0}$ and $\Delta L_{p4,0}$, Strategy 2.

cases higher ΔV solutions are obtained at low values of $\Delta L_{a4,0}$. For all the points that converged, the solutions are all different from each other, showing that the problem is characterised by a high number of local minima. The results shown in Fig. 2 to 5 are obtained using an initial guess for the elevation angle equal to zero (Eq. 13). The next step is to solve a local optimisation problem using as initial guess for ΔL_{p4} and ΔL_{a4} the initial guess of the solution corresponding to the lower ΔV in Fig. 2 to 5, and with values of the initial guesses of the elevation angles different from zero. The initial guess vector is now expressed

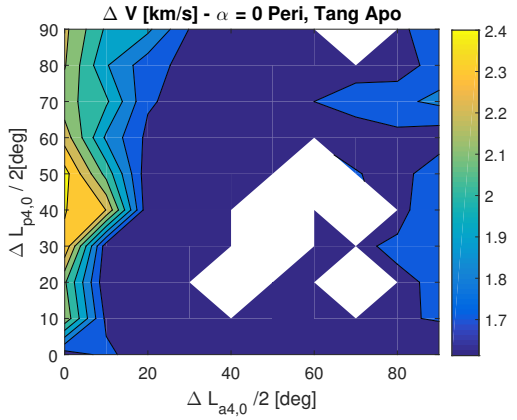

Fig. 4. ΔV for different initial guesses of $\Delta L_{a4,0}$ and $\Delta L_{p4,0}$, Strategy 3.

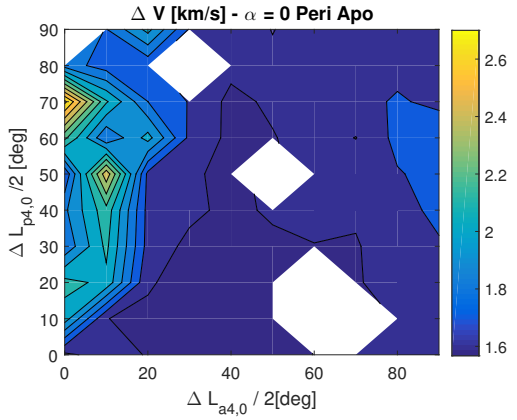

Fig. 5. ΔV for different initial guesses of $\Delta L_{a4,0}$ and $\Delta L_{p4,0}$, Strategy 4.

as:

$$\mathbf{x}_0 = [0\ 0\ 0\ \ -\Delta L_{p4,0}^{min\Delta V}\ 0\ \frac{L_{a4,0}^{min\Delta V}}{3}\ \frac{2\Delta L_{a4,0}^{min\Delta V}}{3}\ \Delta L_{a4,0}^{min\Delta V}$$
$$\beta_{p0}\ \beta_{p0}\ \beta_{p0}\ \beta_{p0}\ \frac{\beta_{a0}}{2}\ \beta_{a0}\ \beta_{a0}\ \frac{\beta_{a0}}{2}]^T \quad (15)$$

where $\Delta L_{p4,0}^{min\Delta V}$ and $\Delta L_{a4,0}^{min\Delta V}$ are the parameters corresponding to the minimum ΔV solution. Fig. 6 to 9 show the results when changing β_{p0} and β_{a0} from 0 to $\pi/2$. Results show that the

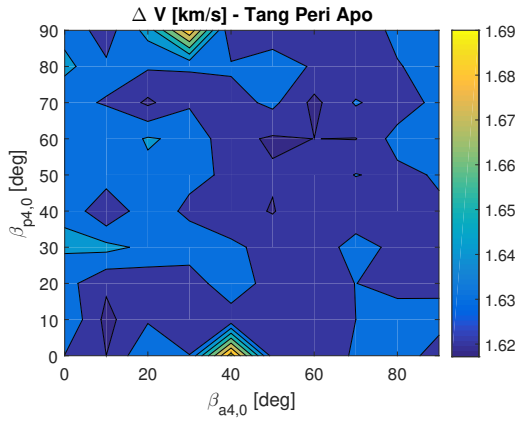

Fig. 6. ΔV for different initial guesses of β_{a0} and β_{p0}, Strategy 1.

effect of the initial guess of the elevation angle on the final solution is limited with respect to the effect of the length of the perigee and apogee thrust arcs. The minimum ΔV solutions are

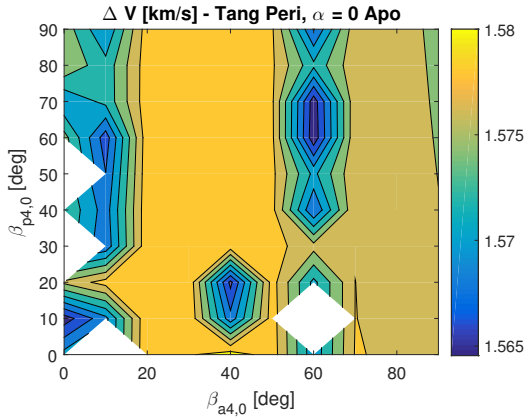

Fig. 7. ΔV for different initial guesses of β_{a0} and β_{p0}, Strategy 2.

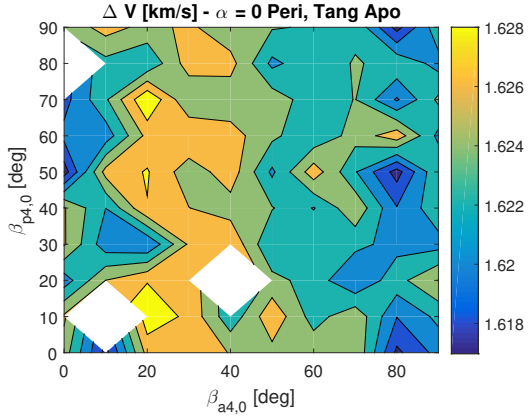

Fig. 8. ΔV for different initial guesses of β_{a0} and β_{p0}, Strategy 3.

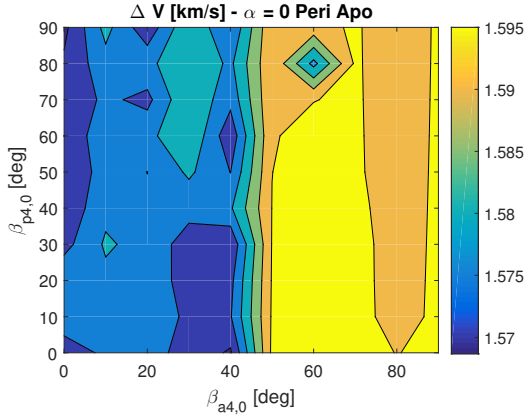

Fig. 9. ΔV for different initial guesses of β_{a0} and β_{p0}, Strategy 4.

Table 2. Minimum ΔV solution for GTO-GEO transfer with no perturbations.

Strategy	1	2	3	4
ΔV [km/s]	1.6172	1.5645	1.6170	1.5687

summarised in Table 2 and show that the best results are given by Strategy 2 and Strategy 4.

The results presented above are obtained solving a local minimisation problem and using a predefined specific expression for the initial guess. Each solution is therefore likely to be a local minima of the problem and might be strongly dependent on the choice of the initial guess. In the following, the results found using the global optimisation algorithm MP-AIDEA are presented. The local search in MP-AIDEA is performed with

MATLAB *fmincon-sqp*. MP-AIDEA is run with 1 population of 16 individuals (dimension of the problem) and for a total of 1.5 10^5 function evaluations; 25 independent runs are considered in order to obtain statistically significant results. The results are shown in Fig. 10 to Fig. 13, for the four considered thrusting strategies. For each strategy, the minimum ΔV for each one of the 25 runs of MP-AIDEA is represented. Three possible values of w_1 and w_2 are considered: 1, 10 and 100. The results of the local optimisation method (Table 2) are represented by the black lines. Results show that the local optimisation method outperforms MP-AIDEA when the initial guess vector is close to the solution of the problem (Fig. 10) while Fig. 13 shows a case in which the global search capabilites of

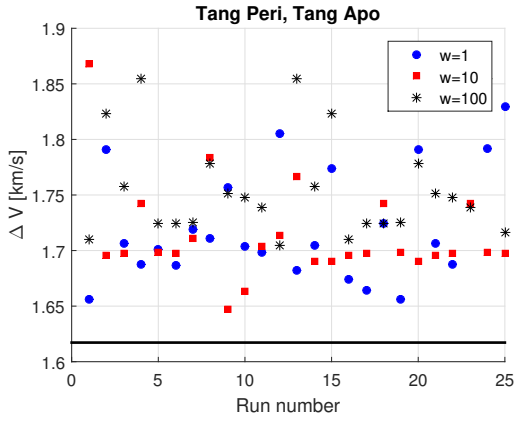

Fig. 10. Minimum ΔV of 25 runs of MP-AIDEA - Strategy 1.

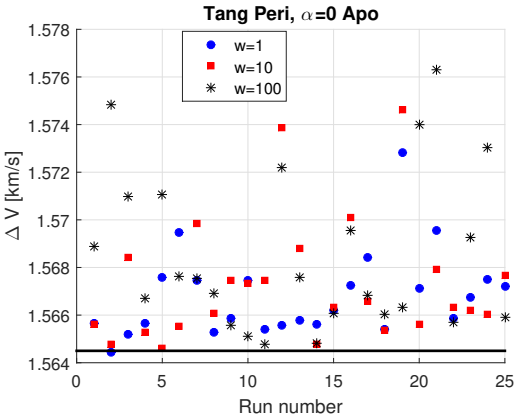

Fig. 11. Minimum ΔV of 25 runs of MP-AIDEA - Strategy 2.

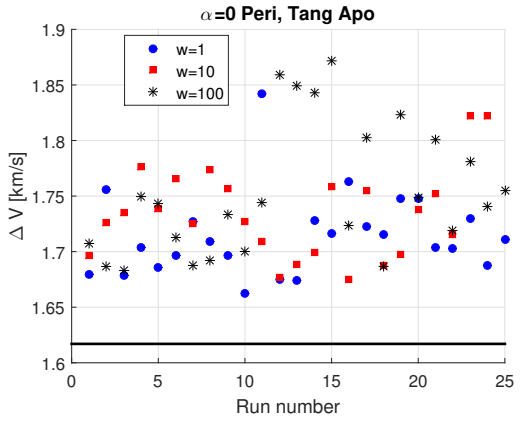

Fig. 12. Minimum ΔV of 25 runs of MP-AIDEA - Strategy 3.

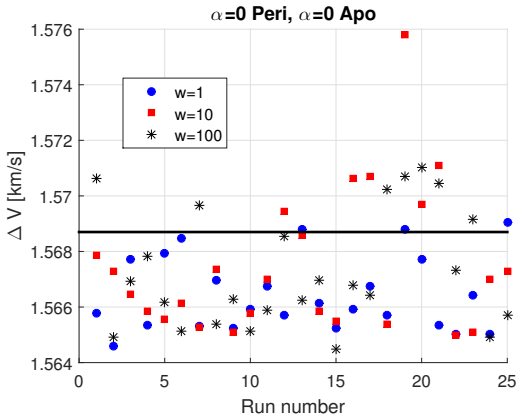

Fig. 13. Minimum ΔV of 25 runs of MP-AIDEA - Strategy 4.

MP-AIDEA are able to locate better solutions than those found by the local optimisation method. The minimum, maximum and mean values of the 25 runs, for each strategy, are reported in Table 3. The minimum ΔV solutions are obtained using Strategy 2 and $w = 1$ and Strategy 4 and $w = 100$ (results in bold in Table 3). The variation of orbital elements and the control parameters during the transfer for these two cases are shown in Fig. 14. r_p and r_a in Fig. 14 are the perigee and apogee radius. Fig. 15 shows the x-y view of the trajectory for Strategy 4. To make the plot more readable, only few orbital revolutions are represented. The thrust arcs are represented by thick black lines.

Table 3. ΔV [km/s] - Results from MP-AIDEA.

	w	Min	Mean	Max
Strat. 1	1	1.6558	1.7263	1.8497
	10	1.6473	1.7129	1.8683
	100	1.7046	1.7580	1.8551
Strat. 2	1	**1.5644**	1.5668	1.5728
	10	1.5646	1.5673	1.5746
	100	1.5648	1.5685	1.5763
Strat. 3	1	1.6626	1.7144	1.8424
	10	1.6747	1.7342	1.8223
	100	1.6833	1.7538	1.8715
Strat. 4	1	1.5646	1.5665	1.5691
	10	1.5650	1.5675	1.5758
	100	**1.5645**	1.5673	1.5710

Each one of the 25 runs of MP-AIDEA provides different solutions to the GTO-GEO transfer problem. As an example, Fig. 16 shows the solutions characterised by $\Delta V < 1.7$ km/s found by a single run of MP-AIDEA using Strategy 4 and $w = 100$. Each solution correspond to different control history and orbital elements variation to realise the GTO-GEO transfer. In particular in this case 233 solutions are found with $\Delta V < 1.7$ km/s, among which 120 with $\Delta V < 1.65$ km/s and 21 with $\Delta V < 1.6$ km/s. The orbital elements variation and control history of the 21 solutions with $\Delta V < 1.6$ km/s are shown in Fig. 17 and 18. A single run of MP-AIDEA can therefore find many local optima and many possible solutions to the problem.

4. GTO-GEO transfer with perturbations

The results presented in the previous section do not consider perturbations to the motion of the spacecraft. In this section the

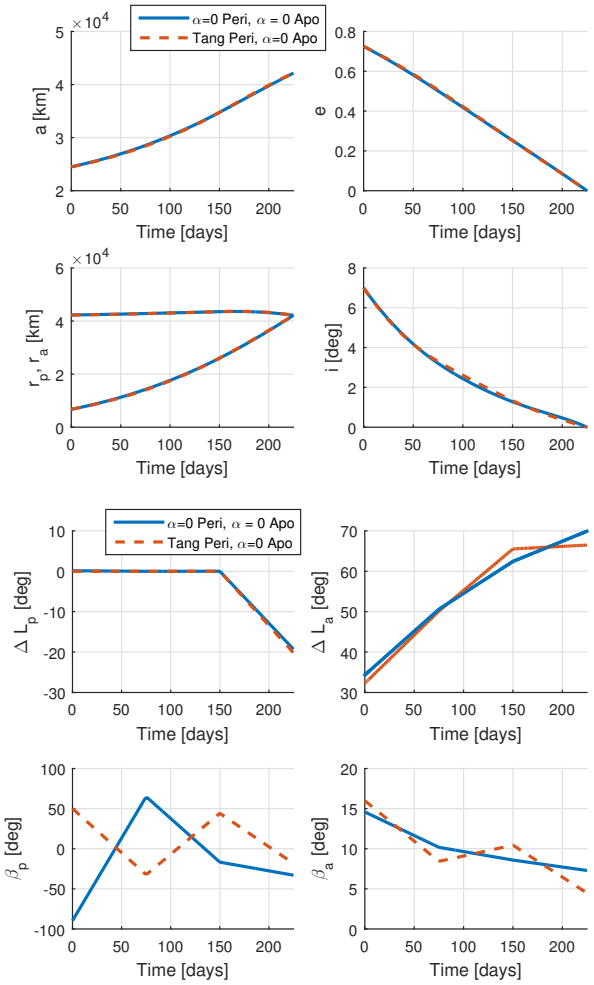

Fig. 14. Orbital elements variation and control history during the GTO-GEO transfer without perturbations - Minimum ΔV solutions from Table 3.

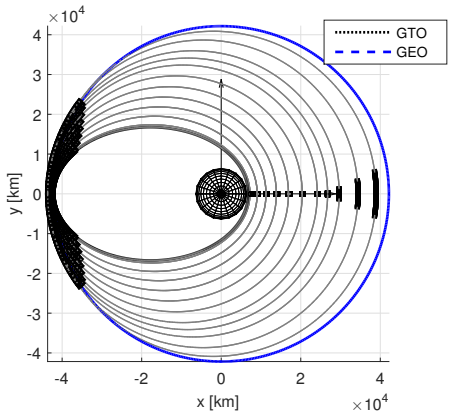

Fig. 15. Minimum ΔV GTO-GEO transfer - Strategy 4.

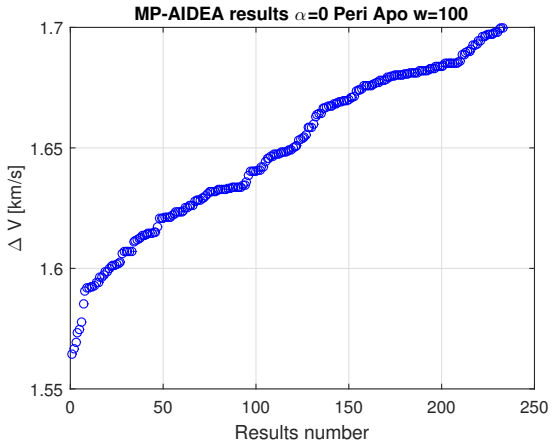

Fig. 16. MP-AIDEA: solutions with ΔV <1.7 km/s using Strategy 4.

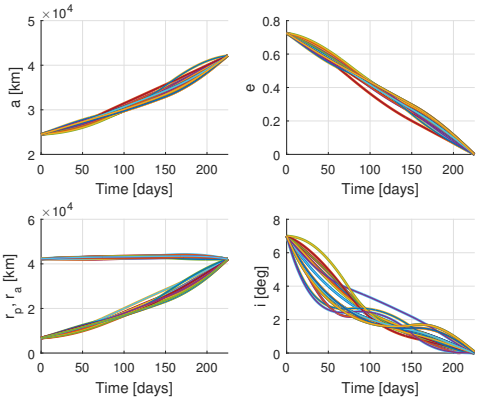

Fig. 17. Orbital elements variation of the 21 solutions of MP-AIDEA characterised by ΔV < 1.6 km/s - Strategy 4.

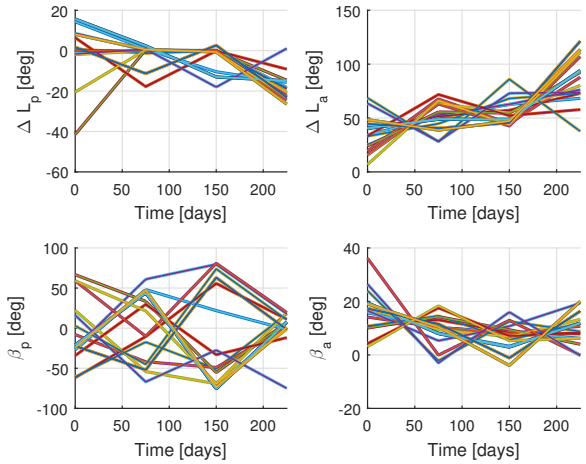

Fig. 18. Control history of the 21 solutions of MP-AIDEA characterised by ΔV < 1.6 km/s - Strategy 4.

perturbations due to Earth's potential, drag and third body are taken into account. Only strategy 4, that together with strategy 2 provided the best results in the case without perturbations, is considered.

4.1. Earth's gravitation perturbations

This section starts presenting the results that justify the need to add two thrust arcs to the control profile when perturbations that change ω are present, as anticipated in Section **2.**. Let us consider the minimum ΔV solution of Section **3.**, given by MP-AIDEA using strategy 4 and $\omega_0 = 0$. This solution is used as initial guess for the local optimisation of the GTO-GEO transfer with the addition of the perturbation due to second zonal harmonic of the aspheric Earth's potential, J_2. The orbital elements and control history are shown in Fig. 19 and 20. The cost of the transfer is $\Delta V = 1.7347$ km/s. Fig. 19 shows that

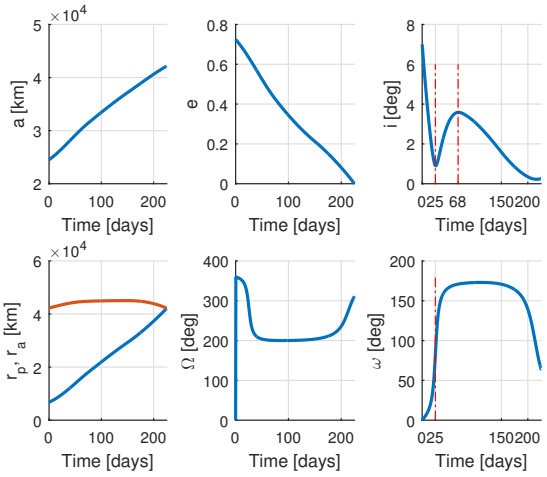

Fig. 19. Orbital elements variation, J_2 and two thrust arcs.

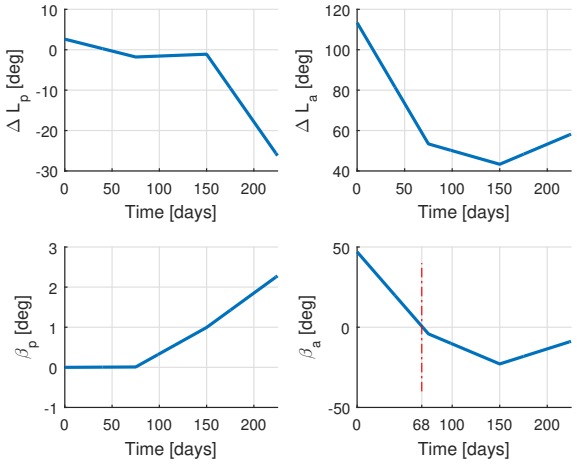

Fig. 20. Control history, J_2 and two thrust arcs.

there is an increase of inclination during the transfer from t = 25 days to t = 68 days. The reason for this behavior is explained in the following. At t = 25 days the argument of perigee (that changes both because of J_2 and because of the low-thrust acceleration) goes from $\omega < \pi/2$ to $\omega > \pi/2$. The Gauss' equation for the time variation of the inclination depends on the term $\sin\beta\cos(\omega+\theta)$; this means that in order to have a continuous reduction of inclination with thrust applied on perigee ($\theta = 0$) and apogee ($\theta = \pi$) centered thrust arcs, β_a should be $\beta_a > 0$ when $\omega < \pi/2$ and $\beta_a < 0$ when $\omega > \pi/2$. Therefore an instantanoues variation in the sign of β_a should take place at t = 25 days. Due to the type of control parametrisation and number of nodes used, the variation in the sign of β_a takes place however at t= 68 days, rather than 25 days (Fig. 20). This explains the increase in inclination from 25 to 68 days from the start of the transfer. At t =68 days the inclination starts to decrease again. This behaviour shows that the control parametrisation used in the previous section requires some changes when considering the perturbation due to J_2, if period of increase of inclination are to be avoided during the transfer. In particular, since ω changes during the transfer when perturbations are considered, the optimal point for the variation of i continuously changes during the transfer (Eq. 3). In order to allow for a reduction of inclination at any value of ω, two additional thrust arcs are added to the control parametrisation. They are characterised by length ΔL_{pa} (thrust arc between perigee and apogee) and ΔL_{ap} (thrust arc between apogee and perigee). The angular distance between any two arcs is constrained to be:

$$\frac{2\pi - \Delta L_p - \Delta L_{pa} - \Delta L_a - \Delta L_{ap}}{4} \tag{16}$$

The elevation angles on the two additional arcs is chosen such as to always cause a decrease of inclination, according to:

$$\beta_{ap} = \beta_{pa} = -\frac{\pi}{2}\mathrm{sgn}\left(\cos(\omega+\theta)\right) \tag{17}$$

The control parameters are now 24, instead of 16:

$$\begin{aligned}\mathbf{x} = [&\Delta L_{p1}\ \Delta L_{p2}\ \Delta L_{p3}\ \Delta L_{p4}\ \Delta L_{a1}\ \Delta L_{a2}\ \Delta L_{a3}\ \Delta L_{a4}\\ &\beta_{p1}\ \beta_{p2}\ \beta_{p3}\ \beta_{p4}\ \beta_{a1}\ \beta_{a2}\ \beta_{a3}\ \beta_{a4}\ \Delta L_{pa1}\ \Delta L_{pa2}\\ &\Delta L_{pa3}\ \Delta L_{pa4}\ \Delta L_{ap1}\ \Delta L_{ap2}\ \Delta L_{ap3}\ \Delta L_{ap4}]^T\end{aligned} \tag{18}$$

The disequality constraint $g_2(\mathbf{x})$ in Eq. 7 is now formulated as:

$$g_2(\mathbf{x}) = \max\left(||\Delta L_p(t)|| + ||\Delta L_a(t)||||\Delta L_{pa}(t)|| + ||\Delta L_{ap}(t)||\right) - 2\pi \tag{19}$$

This new parametrisation of the control is used to solve the GTO-GEO transfer with perturbations due to J_2. As in the previous section, at first a local optimisation process is considered. The initial guess for ΔL_p, ΔL_a, β_p and β_a are the results of the best solution of the previous section. For ΔL_{pa} and ΔL_{ap} the value of their initial guess is taken in the range 0 to 180 deg. The results of the local optimisation of the problem, starting from different initial guess for ΔL_{pa} and ΔL_{ap}, are shown in Fig. 21. The minimum ΔV solution is represented in Fig. 22

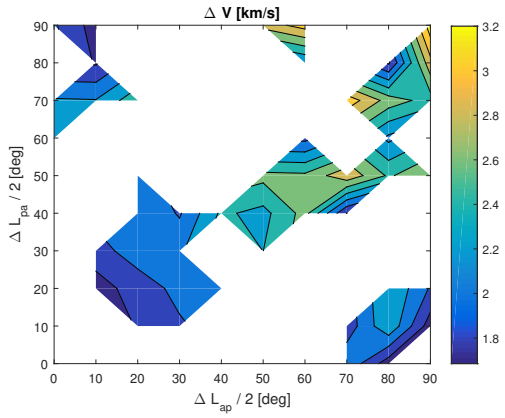

Fig. 21. ΔV for transfer with J_2 perturbations for different values of the initial guess of ΔL_{ap} and ΔL_{pa}, $\omega_0 = 0$

and Fig. 23. The cost of the transfer is ΔV = 1.6848 km/s, lower than the cost of 1.7347 km/s found with two thrust arcs, and the inclination decreases during the entire transfer. Results show that the additional thrust arcs have non-negligible semi-amplitude only in the last phase of the transfer (t > 150 days) when indeed the value of ω approaches 90 deg, and therefore it is not efficient to change the inclination in the vicinity of the perigee and apogee of the orbit (Fig. 23). The solution has been validated by comparing it to the results of a numerical integration of the equations of motion using the control profile defined in Fig. 23. The comparison between numerical and analytic integration is shown in Fig. 24 and shows the good

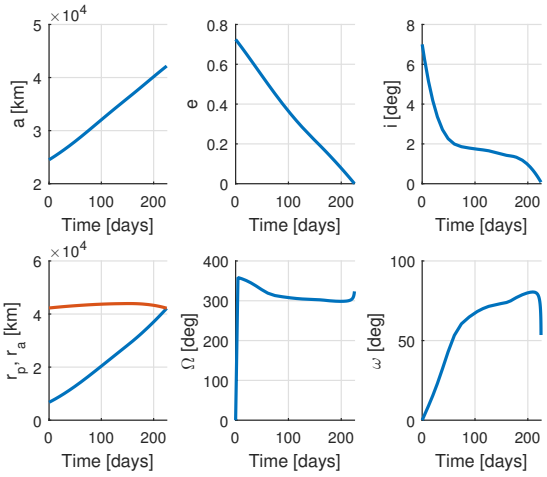

Fig. 22. Variation of orbital elements from local optimisation: J_2, 4 thrust arcs, $\omega_0 = 0$.

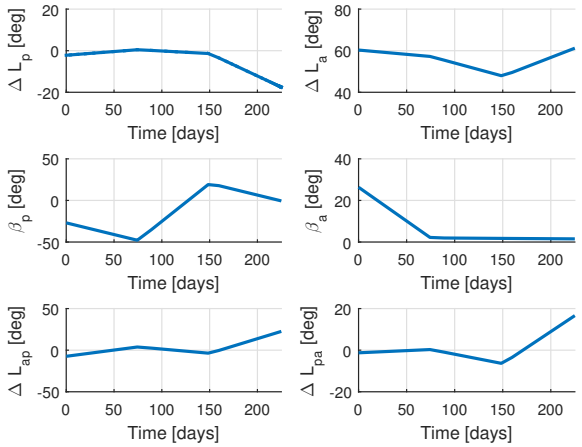

Fig. 23. Control history from local optimisation:J_2, 4 thrust arcs, $\omega_0 = 0$.

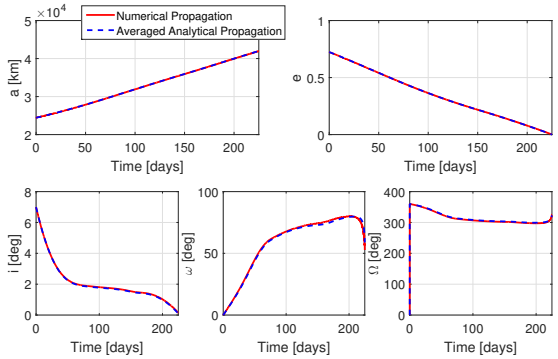

Fig. 24. Numerical and averaged analytical propagation.

agreement between the two models. The optimal solution to the GTO-GEO transfer with J_2 perturbation is sought also using MP-AIDEA. In order to facilitate convergence to the feasible region, the search space is reduced with respect to the one presented in Eq. (8). The new boundaries for the search space are $\Delta L_{pi} \in [-\pi/4, \pi/4]$, $\Delta L_{ai} \in [0, \pi/2]$, $\beta_{pi}, \beta_{ai} \in [-\pi/2, \pi/2]$ and $\Delta L_{pai}, \Delta L_{api} \in [-\pi/4, \pi/4]$. MP-AIDEA is now run with 1 population of 24 individuals. The cost of the feasible solutions found by one run of MP-AIDEA are shown in Fig. 25. By comparing Fig. 25 with Fig. 16 it is possible to see that the number of solutions provided by a run of MP-AIDEA is now reduced with respect to the case without perturbations. The minimum cost solution found by MP-AIDEA is $\Delta V = 1.6588$ km/s, lower than the value of 1.6848 km/s found by the local optimisation (black line in Fig. 25). With the additions of perturbations, the

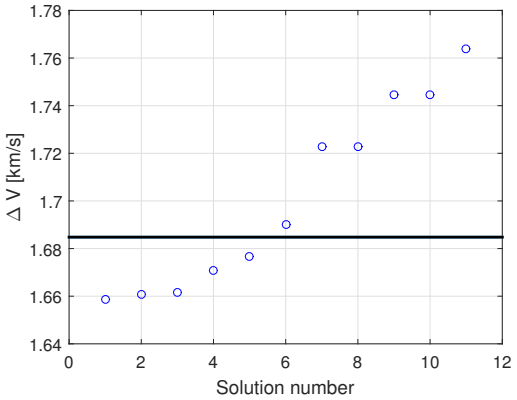

Fig. 25. ΔV of feasible solution found by MP-AIDEA for GTO-GEO transfer with J2 perturbations and $\omega_0 = 0$.

initial value of ω of the GTO plays an important role. Therefore the analysis presented above, valid for $\omega_0 = 0$ is realised also for $\omega_0 = 178$ deg, the initial value of ω for the GTO of the Ariane launcher †. Fig. 26 shows the results of the solution of several local optimisation problem with initial guess given by the solution without J_2 and $\omega_0 = 0$ and using values for the initial guess of ΔL_{pa} and ΔL_{ap} in the range from 0 to π. The minimum ΔV solution found by local optimisation is rep-

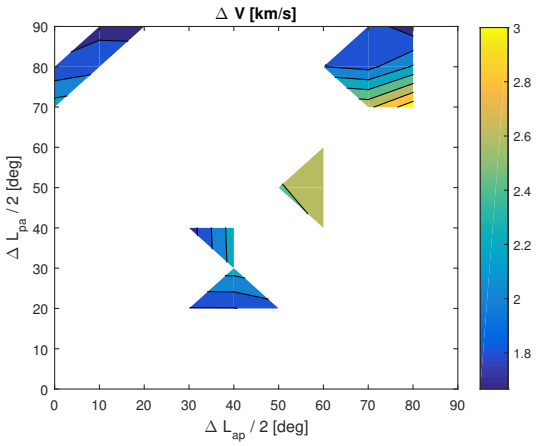

Fig. 26. ΔV for transfer with J_2 perturbations for different values of the initial guess of ΔL_{ap} and ΔL_{pa}, $\omega_0 = 178$ deg.

resented in Fig. 27 and 28 and is characterised by $\Delta V = 1.6668$ km/s. The cost of the feasible solutions found by one run of MP-AIDEA are shown in Fig. 29, together with a black line representing the minimum ΔV solution found by local optimisation. The orbital elements variation of the five solutions with lower ΔV are shown in Fig. 30. The minimum cost solution found by MP-AIDEA has $\Delta V = 1.6452$ km/s, lower than the solution of the local optimisation method. The minimum ΔV

† http://www.arianespace.com/wp-content/uploads/2011/07/Ariane5_Users-Manual_October2016.pdf

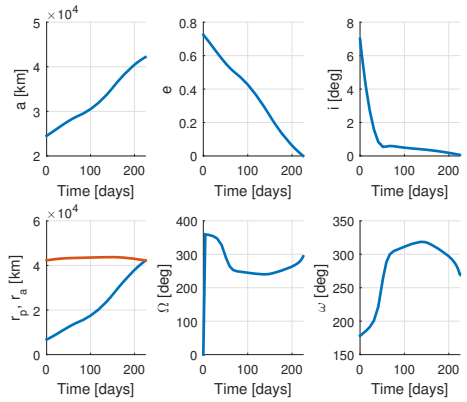

Fig. 27. Variation of orbital elements from local optimisation: J_2, 4arcs, ω_0 = 178 deg.

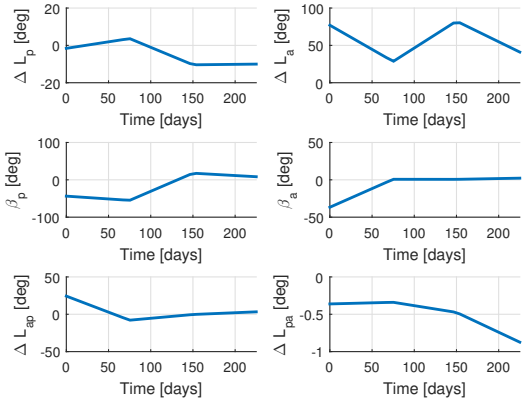

Fig. 28. Control history from local optimisation: J_2, 4 thrust arcs, ω_0 = 178 deg.

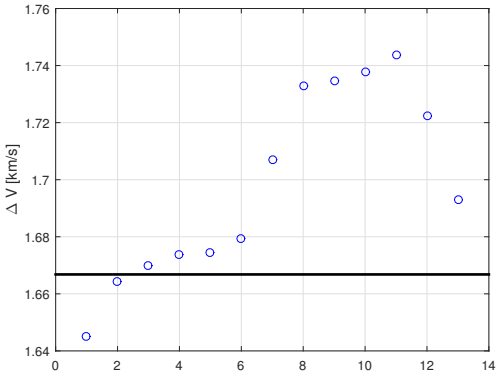

Fig. 29. ΔV of feasible solutions found by MP-AIDEA for GTO-GEO transfer with J_2 perturbations and ω_0 = 178 deg.

solution is analysed in more detail to study the effect of additional perturbations: J_3, J_4 and J_5. No significant difference in ΔV is evident when considering these additional perturbations and the profile of the variation of the orbital elements remains approximately the same. In more detail, the ΔV and orbital elements at the end of the transfers are reported in Table 4.

4.2. Atmospheric drag

In this subsection the effect of the atmospheric drag is analysed. The considered atmospheric model is a static exponential model with zero density of the atmosphere at altitude higher

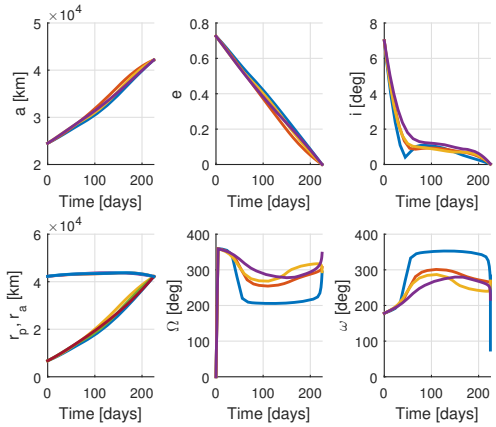

Fig. 30. Orbital element variation of the 5 best solutions found by MP-AIDEA for GTO-GEO transfer with J_2 perturbations and ω_0 = 178 deg.

Table 4. Final orbital element and ΔV - Effect of the Earth's perturbation

	J_2	J_2, J_3	J_2, J_3, J_4	J_2, J_3, J_4, J_5
a [km]	42166.42	42166.34	42166.32	42166.32
e	1.41e-5	1.62e-5	1.68e-5	1.67e-5
i [deg]	0.03	0.03	0.03	0.03
ΔV [km/s]	1.6452	1.6452	1.6452	1.6452

than 4000 km.[4, 12] No significant difference is measured when considering the perturbation due to the atmospheric drag for area to mass ratio of the spacecraft with typical values of 10^{-2} m^2/kg, as shown in Table 5. Table 5 shows the final orbital elements considering the optimal control profile defined in Subsection **4.1.** and J_2, J_3, J_4, J_5 and the drag perturbation. Results

Table 5. Final orbital elements and ΔV- Effect of the drag perturbation

Parameter	J_2, J_3, J_4, J_5	J_2, J_3, J_4, J_5, drag
a [km]	42166.42	42164.77
e	1.41e-5	1.44e-5
i [deg]	0.03	0.03
ΔV [km/s]	1.6452	1.6452

show that, as expected, when using the control profile computed without the atmospheric drag, the addition of the atmospheric drag causes a reduction of the final semimajor axis. The reduction is however negligible and it is possible to state that the effect of the atmospheric drag is not significant for the considered GTO-GEO transfer.

4.3. Sun's gravitational perturbation

For the analysis of the perturbation due to the Sun, the position of the Sun with respect to the orientation of the GTO orbit, and therefore the initial date of the transfer, has to be taken into account. It is assumed that the spacecraft is injected into the GTO by an Ariane launch from Kourou. Fig. 31 shows the right ascension of the GTO orbit at the opening and closing of the launch windows for each day of the year.[12] The GTO-GEO transfer with J_2 and Sun's perturbation is analysed at four different initial dates using different values of Ω for the GTO orbit, corresponding to the opening time of the launch windows (Table 6). The feasible results of a single run of MP-AIDEA for

Table 6. Initial Ω at different initial dates for the transfer

Date	21 March	21 June	21 Sept.	21 Dec.
Ω_0 [deg]	332.05	55.23	148.92	240.87

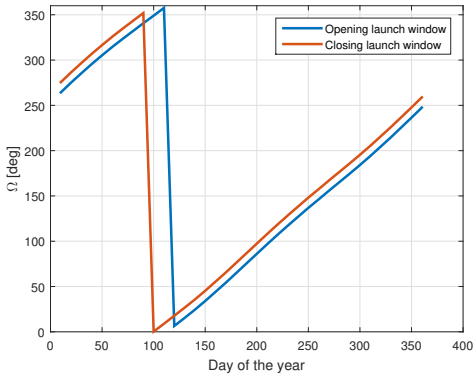

Fig. 31. Variation of Ω of the GTO orbit during the year.

different initial dates are shown in Fig. 32 . The black line represent the result of MP-AIDEA without the perturbation from the Sun (ΔV = 1.6452 km/s). The final orbital elements at the

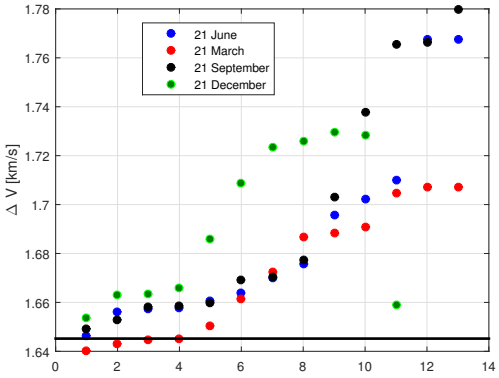

Fig. 32. ΔV of the solution found by MP-AIDEA for transfer with J_2 and Sun perturbation.

end of the transfer and the ΔV of the best solution found for each one of the four considered dates are reported in Table 7.

Table 7. Final orbital elements and ΔV - Sun's gravitational perturbation

	21 March	21 June	21 Sept.	21 Dec.
a [km]	42166.26	42168.89	42165.05	42166.42
e	5.29e-5	4.12e-4	2.23e-5	1.11e-4
i [deg]	0.008	0.06	3.64e-4	0.02
ΔV [km/s]	1.6403	1.6463	1.6494	1.6536

5. Conclusion

This paper presented the results of the global optimisation of the low-thrust transfer from GTO to GEO, including different types of perturbation. Results have shown that a global optimisation method can explore the solution space and locate better solutions than a local optimisation method, without the need to provide an initial guess to the solution. The addition of perturbations can cause differences in the results. In particular, the main difference with respect to the Keplerian case are caused by J_2; however also the Sun's perturbation can cause small but non negligible difference in the cost of the transfer.

References

1) Battin, R. H.: *An introduction to the mathematics and methods of astrodynamics*, AIAA, 1987
2) Dachwald, B.: *Optimization of very-low-thrust trajectories using evolutionary neurocontrol*, Acta Astronautica, Vol. 57 (2005), pp. 175-185.
3) Di Carlo, M., Vasile, M., Minisci, E.: *Multi-population inflationary differnetial evolution algorithm with adaptive local restart*, 2015 IEEE Congress on Evolutionary Computation (CEC), 25-28 May 2015, Japan.
4) Di Carlo, M., Romero Martin, J. M., Vasile, M.: *Automatic trajectory planning for low-thrust active removal mission in Low-Earth Orbit*, Advances in Space Research, Vol. 59, No. 1 (2017), pp. 1234-1258
5) Graham, K. F., Rao, A. V.: *Minimum-Time Trajectory Optimization of Multiple Revolution Low-Thrust Earth-Orbit Transfers*, Journal of Spacecraft and Rockets, Vol. 52, No. 3 (2015), pp. 711-727
6) Kluever, C. A., Oleson, S. R.: *Direct Approach for Computing Near-Optimal Low-Thrust Earth-Orbit Tansfers*, Cambridge University Press, London, 1967, pp.1–10.
7) Kluever, C. A.: *Geostationary Orbit Transfers Using Solar Electric Propulsion with Specific Impulse Modulation*, Journal of Spacecraft and Rockets, Vol. 41, No. 3 (2004), pp. 461-466.
8) Koppel, C. R.: *Advantages of a continuous thrust strategy from a geosynchronous transfer orbit, using high specific impulse thrusters*, 14th International Symposium on Space Flight Dynamics, 8-12 February 1999, Brazil.
9) Petropolous, A. E., Longuski, J. M.: *Shape-Based Algorithm for Automated Design of Low-Thrust, Gravity-Assist Trajectories*, Journal of Spacecraft and Rockets, Vol. 41, No. 5 (2004), pp. 787-796
10) Ruggiero, A., Pergola, P., Marcuccio, S., Andrenucci, M.: *Low-Thrust Maneuvers for the Efficient Correction of Orbital Elements*, 32nd International Electric Propulsion Conference, 11-15 September 2011, Germany.
11) Storn, R., Price, K.: *Differential Evolution: a Simple and Efficient Heuristic for Global Optimization over Continuous Spaces*, Journal of Global Optimization, Vol. 11, No. 4 (1997), pp. 341-359
12) Vallado, D. A.: *Fundamentals of Astrodynamics and Applications*, Ed. Springer, 2007
13) Vasile, M.: *A Global Approach to Optimal Space Trajectory Design*, 13th AAS/AIAA Space Flight Mechanics Meeting, 9-13 February 2003, Puerto Rico.
14) Wales, D. J, Doye, J. P. K.:*Global Optimization by Basin-Hopping and the Lowest Energy Structures of Lennard-Jones Clusters Containing up to 100 Atoms*, Journal of Phys. Chem. A, Vol 101, No. 28 (1997), pp. 5111-5116
15) Williams, S. N., Coverstone-Carroll, V.: *Benefits of Solar Electric Propulsion for the Next Generation of Planetary Exploration Missions*, Journal of the Astronautical Sciences, Vol. 45, No. 2 (1997), pp. 143-159.
16) Yam, C. H, Lorenzo, D., Izzo, D.:*Low-thrust traectory design as a constrained global optimization problem*, Proceedings of the Institution of Mechanical Engineers, Part G: Journal of Aerospace eengineering, 2011
17) Zuiani, F., Vasile, M.: *Extended analytical formulas for the perturbed Keplerian motion under a constant control acceleration*, Celestial Mechanics and Dynamical Astronomy, Vol. 121, No. 3 (2015), pp. 275-300